6
AN ANALYSIS OF MULTI-PASS OVERLAYS

6.1 INTRODUCTION

The mechanisms that affect dilution in multi-pass overlays are more complex than those affecting the dilution of single-bead deposits. As was seen in section 2.2.1, the dilution of a single bead is defined by two quantities: the volume of material that is deposited and the volume of substrate that is melted. In a multi-pass overlay, however, a bead is generally formed by the melting and mixing of three materials, namely:

- the welding consumable,
- the substrate material, and
- the previous bead.

The purpose of this chapter is to develop a model of dilution for multi-pass overlays.

6.2 DEVELOPMENT OF A MODEL

6.2.1 Definition of Variables

It is helpful to consider a bead in a multi-pass overlay in terms of three area fractions. The area fractions of a bead in a multi-pass overlay are represented schematically in Figure 6.1. The first, denoted k, refers to the area fraction of the bead contributed by material deposited in that pass. The second, denoted $\square$, represents the area fraction of the bead contributed by material from the previous bead. The third fraction is the

contribution of new substrate material. Since the three fractions must sum to unity, the substrate fraction can be expressed in terms of k and γ as follows:

$$substrate\ fraction = 1 - k - \gamma \quad \ldots\ldots \quad (6.1)$$

As k and γ are fractions they must also satisfy the following inequality:

$$k + \gamma \geq 1 \quad \ldots\ldots\ldots (6.2)$$

In equation 6.2 equality occurs if no substrate material is melted. Such an event may occur if one bead is deposited directly on top of another.

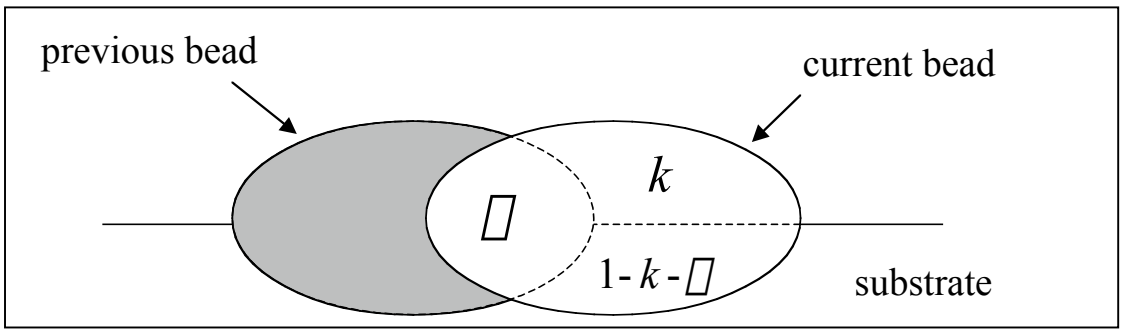

Figure 6.1: - Schematic representation of a bead in a multi-pass overlay.

It is worth noting that for a single-bead deposit $\gamma = 0$ as there is no previous bead present. In this case k assumes a value equal to the complement of the single-bead dilution, D_{sb}, *i.e.*:

$$k = 1 - D_{sb} \quad \ldots\ldots\ldots \quad (6.3) \quad (\text{single-bead deposit})$$

6.2.2. Definition of Problem

Consider the case where the following ***conditions*** apply:

1) A single-layer overlay is deposited with the welding parameters being identical for each pass.
2) The all-weld-metal composition and the base material composition are different.
3) The inter-pass temperature is the same for each pass.

In addition, the following simplifying ***assumptions*** will be made:

1) Each bead in the overlay is perfectly homogeneous.
2) The total cross-sectional area of material melted is the same for each bead in the overlay and equal to that for a single-bead deposit.
3) k remains unchanged from the first bead and $\square$ remains unchanged from the second bead until a steady-state condition is reached.

6.2.3. Analysis

If these conditions apply then the concentration of alloying element x in the first bead, denoted $[x]_1$, will be given by:

$$[x]_1 = k[x]_{awm} + (1 \square k)[x]_{bm} \quad \ldots\ldots\ldots (6.4)$$

where $[x]_{awm}$ = concentration of element x in an all-weld-metal deposit, and

$[x]_{bm}$ = concentration of element x in the base material.

Equation 6.4 describes the special case of a single-bead deposit where θ = 0 and equation 6.3 applies. Consider now the deposition of a second overlapping bead. The concentration of element *x* in this bead will be given by:

$$[x]_2 = k[x]_{awm} + \theta[x]_1 + (1 - k - \theta)[x]_{bm} \quad \ldots\ldots\ldots (6.5)$$

Substituting equation 6.4 into equation 6.5 and rearranging gives:

$$[x]_2 = [x]_{awm}(k + \varepsilon k) + [x]_{bm}(1 - k - \varepsilon k)$$

A similar approach may be adopted for the third bead to give:

$$[x]_3 = [x]_{awm}(k + \varepsilon k + \varepsilon^2 k) + [x]_{bm}(1 - k - \varepsilon k - \varepsilon^2 k)$$

It can be shown that, if the above conditions and assumptions apply, the concentration of element *x* in the N^{th} bead of an overlay, $[x]_N$, will be given by:

$$[x]_N = [x]_{bm} + k([x]_{awm} - [x]_{bm}) \sum_{j=0}^{N-1} \varepsilon^j \quad \ldots\ldots\ldots (6.6)$$

This equation will provide an estimate of the concentration of any element in any bead in the overlay, from the first bead deposited through to the steady-state condition. The sum in equation 6.6 is a geometric series and, as *N* becomes large, the sum converges to a limiting value, *i.e.*:

$$\sum_{j=0} \varepsilon^j = \frac{1}{1 - \varepsilon} \quad \ldots\ldots\ldots (6.7)$$

Consequently, an expression can be written for the steady-state concentration of any element, $[x]_{ss}$, in the overlay:

$$[x]_{ss} = [x]_{bm} + \frac{k}{1-\gamma}\left([x]_{awm} - [x]_{bm}\right) \quad \ldots\ldots\ldots (6.8)$$

Equations 6.6 and 6.8 will reveal a great deal of information about single-layer overlays provided values can be obtained for k and γ. A value for k can be obtained by combining equation 6.3 with the model for single-bead dilution (see equation 2.2 – page 10) proposed by Bednarz (1996) and reported in Francis *et al.* (1998). An estimate for γ, the area fraction of overlap, is more difficult to obtain. It is helpful, however, to consider how γ may vary as a function of the bead overlap, δ. Bead overlap is normally defined in terms of the single-bead width, w, and the step-over or offset between adjacent weld beads, Δ. The bead overlap is given by:

$$\delta = 1 - \frac{\Delta}{w} \quad , \quad 0 \le \delta \le 1 \quad \ldots\ldots\ldots (6.9)$$

If the step-over is equal to the bead width then the overlap, δ, is zero. It can be appreciated that if the overlap is equal to zero there can be no area fraction of overlap. Thus one boundary condition for $\gamma = f(\delta)$ becomes:

$$f(0) = 0 \quad \ldots\ldots\ldots (6.10)$$

If the step-over is zero, the overlap, δ, is equal to unity. This condition is equivalent to depositing one bead directly on top of its predecessor. One would not expect any additional or new substrate to be melted under these circumstances. Consequently, the substrate fraction, defined by equation 6.1 is equal to zero at 100% overlap, *i.e.*:

$$1 - k - \Gamma = 0$$

This relationship can be rearranged to provide the other boundary condition for $\Gamma = \Gamma(\Delta)$.

$$\Gamma(1) = 1 - k \quad \ldots\ldots\ldots (6.11)$$

Equations 6.10 and 6.11 provide the end conditions for the unknown function $\Gamma = \Gamma(\Delta)$. A first order approximation to the function is a straight line between the two end points, *i.e.*:

$$\Gamma = \Gamma(1 - k) \quad \ldots\ldots\ldots (6.12)$$

Equation 6.12 satisfies both end-conditions and, together with equations 6.3, 6.6 and 6.8, provides a simple model for multi-pass overlays.

6.3 STEADY-STATE DILUTION FOR Γ LINEAR WITH Δ

One parameter of interest is the predicted steady-state dilution. Consider an overlay in which *N* beads have been deposited. The average dilution of the overlay can be written in terms of the total material that is deposited and the total material that is melted. If assumptions 2 and 3 apply, the average dilution, D_{av}, can be written as:

$$D_{av} = \frac{A(1-k) + A(N-1)(1-k-\ddot{e})}{NkA + A(1-k) + A(N-1)(1-k-\ddot{e})}$$

where *A* is the total cross-sectional area of a bead, and is assumed to be the same for all beads in the overlay. As *N* becomes large this expression approaches the value:

$$D_{av} = \frac{1 - k - \ddot{e}}{1 - \ddot{e}} \quad \text{.....(6.13)}$$

which is an estimate for the steady-state dilution of an overlay. A physical interpretation of this result can be derived by referring to Figure 6.1 (page 107). The numerator of equation 6.13 refers to the substrate fraction, *i.e.* the fraction of the bead contributed by new or previously unmelted substrate. The denominator represents the entire bead minus the component contributed by overlap with the previous bead. Thus equation 6.13 states that the steady-state dilution of an overlay is independent of how much of the previous bead is melted. All that matters is the ratio of material deposited in each pass to the amount of new substrate melted under steady conditions.

6.4 RATE OF CONVERGENCE FOR □ LINEAR WITH □

Consider the deposition of a multi-pass overlay. Let the welding consumable produce an all-weld-metal deposit containing 25wt.% chromium and let the base material be a mild steel containing no chromium. Suppose that the welding conditions are such that a single-bead deposit would have a dilution, D_{sb}, of 50% and that the overlap, □, is also 50%. Thus k will have a value of 0.5 (the complement of the single-bead dilution) and □ will assume a value of 0.25 as required by equation 6.12. Equation 6.6 predicts the chromium concentrations for each bead in the overlay, and the first few results are plotted in Figure 6.2. It can be seen that the chromium concentrations will first assume the value for a single-bead deposit (bead no. 1) and then converge to the steady-state value, given by equation 6.8, of 16.7%. The steady-state dilution, given by equation 6.13, is 33%.

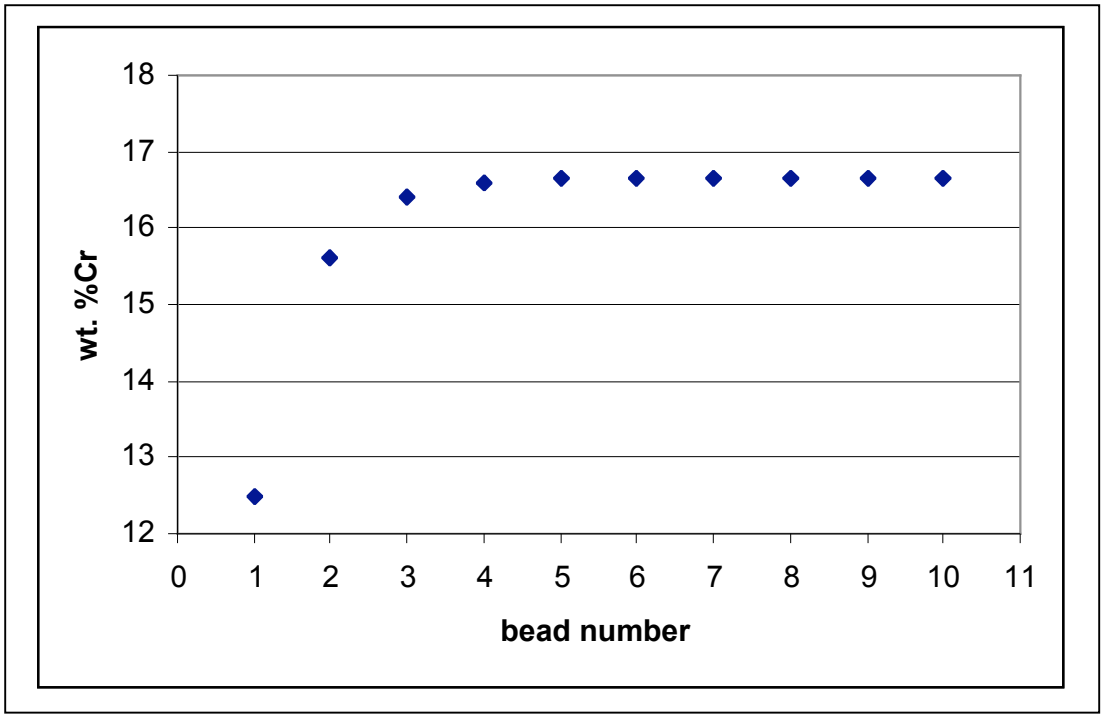

Figure 6.2: - An example of a convergence pattern for chromium concentration as predicted by the *k*-□ model. The chromium concentration in an all-weld-metal deposit was assumed to be 25wt.%, while the substrate was assumed to be chromium-free. It was assumed that the welding conditions would produce a single-bead deposit with 50% dilution. The overlap was also assumed to be 50%.

The form of equation 6.6 suggests that the rate at which the composition converges is independent of *k* and dependent only on □. In practical situations □ will vary between 0 and 0.5; □ will be equal to zero when the overlap is zero and, at the other extreme, □ = 0.5 corresponds to one 50%-dilution single bead being deposited directly on top of another. Figure 6.3 shows the convergence trend for low, moderate and high values of □. Equation 6.8 predicts steady-state chromium concentrations of 12.6%, 16.7% and 25% for □ = 0.01, 0.25 and 0.5 respectively. In all cases it was assumed that $k = 0.5$ and that the welding consumable would produce an all-weld-metal deposit containing 25wt.% chromium. It can be seen that when $k + □ = 1$, as is the case here when □ = 0.5, the overlay composition will converge to the all-weld-metal composition.

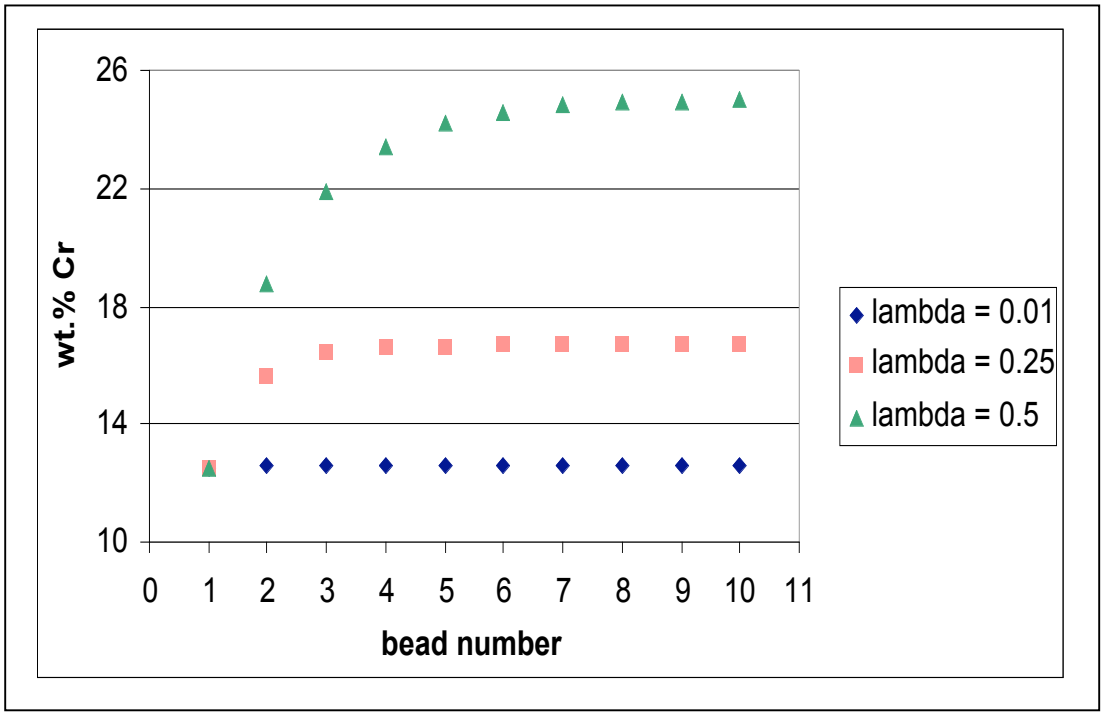

Figure 6.3: - Chromium concentration vs bead number for three different values of λ. The rate of convergence appears to decrease as λ increases. The chromium concentration in an all-weld-metal deposit was assumed to be 25wt.%. The substrate was assumed to contain no chromium. It was assumed that the welding conditions would produce a single-bead deposit with 50% dilution.

Let it be assumed that a steady-state condition has effectively been reached when the composition has reached a value 95% of the way from the single-bead composition to the steady-state composition. That is to say if:

$$\lambda + \lambda^2 + \lambda^3 \ldots\ldots\ldots \geq 0.95\left[\frac{1}{1-\lambda} - 1\right] \quad \ldots\ldots\ldots (6.14)$$

then a steady state is assumed to have been reached (see equations 6.6 and 6.7). It can be seen from Table 6.1 that when $\lambda = 0.01$ convergence occurs after only two beads have been deposited. At the other extreme, it is necessary to deposit six beads in order to achieve convergence when $\lambda = 0.5$. To a first order approximation λ is directly

proportional to bead overlap. Consequently, this model suggests that at low overlaps convergence occurs almost immediately but, as the overlap increases, more beads need to be deposited for convergence to occur.

γ	Value At Which Convergence Is Deemed To Have Been Achieved (see ineq. 6.14)	Value of Sum					
		Bead 1	Bead 2	Bead 3	Bead 4	Bead 5	Bead 6
0.01	0.010	0.000	0.010	0.010	0.010	0.010	0.010
0.25	0.317	0.000	0.250	0.313	0.328	0.332	0.333
0.40	0.633	0.000	0.400	0.560	0.624	0.650	0.660
0.50	0.950	0.000	0.500	0.750	0.875	0.938	0.969

Table 6.1: - The value of the sum $1 + \gamma + \gamma^2 + \gamma^3 + \ldots - 1$ is given as a function of bead number for various γ. The value at which the sum is deemed to have reached a steady state is also given for comparison.

An explanation for the effect of γ on the rate of convergence is given here. The first bead in a multi-pass overlay is unique in that it is deposited in the same manner as a single-bead deposit. It will have a higher dilution than all other beads in the overlay since, in the first pass, the welding consumable is diluted by substrate material alone. All other beads overlap with their predecessors. The first bead, however, influences subsequent beads in the overlay because part of the first bead is melted and mixed into the second bead. Part of the second bead is then melted and mixed into the third bead

etc. Each bead in the overlay is thus mixed, to some extent, with the first (high-dilution) bead. In fact, under the conditions described in section 6.2.2, the fraction of the first bead mixed into the N^{th} bead in the overlay will be γ^{N-1}. It can be seen that, as γ decreases, the influence of the first bead will decay more rapidly, resulting in faster convergence to the steady-state condition.

6.5 A SPREADSHEET FOR PREDICTING DILUTION IN MULTI-PASS OVERLAYS

It is possible, using the theory developed in sections 6.2 to 6.4, to establish a link between the selected welding parameters and the composition of an overlay. In the Australian hardfacing industry, 2.8mm diameter electrodes are preferred together with the direct-current, electrode-positive (DCEP) configuration. The larger consumable diameter facilitates a higher deposition rate and, due to the desirable metal transfer characteristics, most consumables are designed for DCEP operation. As for single-bead deposits, down-hand deposition is the preferred mode of operation and, consequently, this analysis applies to this configuration. This leaves voltage, V, current, I, work distance, l, and travel speed, S at the discretion of the operator. Once these variables have been selected the step-over, γ, is immediately defined in that the specified overlay height has been pre-determined by the end-user. There will be only one step-over that achieves the specified overlay height and that can be determined using equation 5.5 (page 98).

For a given combination of voltage, current, work distance and travel speed it is possible to estimate the single-bead dilution using equation 2.2 (page 10). If the conditions and assumptions described in section 6.2.2 apply, the calculated single-bead dilution can be used to estimate k, the deposited fraction of the bead. All that remains is to estimate γ.

A first approximation to λ is obtainable from equation 6.12 in terms of k, already known, and the overlap, ψ. The bead overlap is a function of the bead width and the step-over. The step-over is obtained from equation 5.5 (page 98) and the bead width from equation 3.4 (page 44) so that ψ can also be estimated. A summary of the algorithm is presented here. The relevant equation numbers are included in parentheses.

SUMMARY OF ALGORITHM

1. *Select* V, I, l, S *and desired steady state overlay height,* H_{ss}.
2. *Calculate* W *from* $W = aI + bII^2$ (2.4)
3. *Calculate* α *from* $\alpha = \dfrac{W}{\psi H_{ss} S}$ (5.5)
4. *Estimate* w *from* $w = \dfrac{C_1}{S} + C_2 VI$ (3.4)
5. *Estimate* ψ *from* $\psi = 1 - \dfrac{\alpha}{w}$ (6.9)
6. *Calculate* D_{sb} *from* $\dfrac{D_{sb}}{1 - D_{sb}} = \lambda \dfrac{VI}{W}(1 + \psi VIS)$ (2.2)
7. *Calculate* k *from* $k = 1 - D_{sb}$ (6.3)
8. *Estimate* ε *from* $\varepsilon = \psi(1 - k)$ (6.12)
9. *Calculate %Cr etc. at steady state from equation* (6.8), *i.e.*:

$$[x]_{ss} = [x]_{bm} + \frac{k}{1 - \varepsilon}\left([x]_{awm} - [x]_{bm}\right)$$

Thus for any combination of V, I, l and S it is possible to predict the resulting overlay composition. The predicted composition will not, however, indicate whether the selected parameters are optimal. (In many instances minimum dilution is the objective and the optimal settings would be those that give minimum dilution or the richest overlay composition.) Consequently, it becomes necessary to compare a range of settings in order to identify conditions that are near-optimal. When this need is combined with the complexity of the algorithm the problem becomes amenable to a

spreadsheet program. In a spreadsheet it is possible to change the input parameters and receive instant output. In addition, several sets of conditions can be entered and compared simultaneously. If the user wishes, a matrix of conditions can be entered and the data set can be ranked in order from the richest to leanest overlay (lowest to highest dilution) for the height specified. Optimum conditions are then readily identified. An example of the original spreadsheet program arising from the current work is shown in Figure 6.4. This spreadsheet was generated for consumable B (see section 3.2).

voltage	current	speed (m/s)	work dist (m)	width (m)	D_{sb}	k	step (m)	overlap	□	hr/m^2	%Cr
28	400	0.0150	0.04	0.011	0.51	0.49	0.0038	0.66	0.34	4.89	20.62
30	350	0.0067	0.04	0.014	0.52	0.48	0.0070	0.50	0.26	5.91	18.16
32	350	0.0100	0.03	0.013	0.57	0.43	0.0042	0.68	0.39	6.59	19.62
26	250	0.0050	0.02	0.010	0.55	0.45	0.0049	0.50	0.27	11.26	17.39

Figure 6.4: - The first spreadsheet for 5mm high overlays. It was assumed that an all-weld-metal deposit would contain 25 wt.% chromium. The base material was assumed to be chromium-free.

It can be seen that the spreadsheet has a column headed "hr/m^2". This column contains an estimate of the minimum time required to cover a square metre of the substrate material and is based only on the estimated deposition rate. It also highlights the fact that the deposition time affects labour costs and will influence the selection of parameters.

6.5.1 Generating a Spreadsheet.

It is only possible to generate a spreadsheet for a particular welding consumable if it has been properly characterised. There are two deposition rate constants (a and b), two

parameters for single-bead dilution ($\square$ and $\square$) and two for bead width (C_1 and C_2), all of which must be known for the consumable. Consequently, it is necessary to deposit at least two single beads-on-plate and to measure the width, dilution and deposition rate for each deposited bead. Each bead must be deposited under different welding conditions. Once these data are obtained it is necessary to fit the results to the respective equations to obtain values for the required constants. The spreadsheet can be constructed as soon as these data are available.

Historically, the spreadsheet was put to immediate use. However inconsistencies were found, and they led to the following detailed examination.

6.6 COMPARISON WITH EXPERIMENTS

Eight overlays were deposited on mild steel substrates. The substrates were 25mm thick, and typically 75mm wide and 350mm long. Each overlay contained between six and twelve beads depending on the rate of convergence to a steady state. The nominal steady-state heights of the overlays ranged from 2 to 6mm. For each overlay, a matching single bead was deposited so that data were available for the single-bead dilution and width.

The general aim was to cover a diverse set of operating conditions within a manageable number of samples. At a height of 4mm, both low and high overlap conditions were used. These two overlays were deposited at ambient temperature and then again with an inter-pass temperature of 400^{o}C. Two different welding consumables were used throughout the experiments, although in both cases they were high-chromium, high-carbon type electrodes.

The contact tip-to-work voltage and current were recorded for every pass with the CSIRO welding monitor (Dick, 1991) described in section 3.2. The wire feed rates were recorded with a hand-held wire feed meter. Inter-pass temperatures were recorded by inserting K-type thermocouples into drilled holes in the substrate. The holes were drilled from the reverse side to a depth of 20mm, so that the measurement points were within 5mm of the substrate surface. Another value for inter-pass temperature was obtained by measuring surface temperature with a K-type surface temperature probe. The values obtained from surface measurement were found to agree well with those measured below the substrate surface, although the surface temperature was usually slightly lower due to faster cooling. A summary of the deposition conditions is given in Table 6.2.

Each overlay and single bead was sectioned so that a slice approximately 10mm in thickness was produced. These slices were surface ground and etched with 10% Nital so that the interfaces between the steel substrate and the deposit would be clearly revealed. For the single-bead deposits dilutions were measured by first placing the sample on an optical projector with 10:1 magnification. Each profile was then traced with high quality tracing paper. The profiles were then carefully cut out and weighed so that the dilutions could be determined from the ratio of the weights. For the larger overlay samples, the slices were scanned and recorded in a *TIFF* file format. Magnified images could then be printed and the penetrations measured. The average penetrations were typically measured across four beads in the deposit, from the fifth-last bead to the penultimate bead. This ensured that the steady-state penetration, not the transient penetration, was measured.

Experimental Plan								
Sample No	Sample Type	WFS (m/min)	Volts	Amps	WD (mm)	Speed (mm/min)	Step-over (mm)	IP Temp (^{o}C)
A	2mm pad	2.26	28.0	380	20	900	6.0	Room
B	3mm pad	2.86	28.2	330	40	730	6.0	Room
C	4mm pad	2.67	28.4	360	30	400	8.0	Room
D	4mm pad	2.77	28.3	360	30	400	8.0	400
E	4mm pad	2.74	28.1	380	30	800	4.0	Room
F	4mm pad	2.74	28.1	370	30	800	4.0	400
G	5mm pad	3.13	27.8	370	30	550	5.0	Room
H	6mm pad	3.81	29.9	440	40	400	8.0	Room

Table 6.2: - The experimental plan for eight overlay samples. Two 2.8mm diameter consumables, equivalent to consumables A and B (see section 3.2), were used to deposit these overlays. Inter-pass temperatures are quoted to the nearest 25^{o}C.

In some instances the currents and voltages for corresponding single-bead and overlay deposits differed. For example, as a welding power source warms up, higher currents can sometimes be drawn even if the settings remain unchanged. Such an effect could introduce errors to the predictions of the *k-*□ model. (The model requires values for the single-bead dilution under welding conditions that are identical to those used in the corresponding multi-pass overlay.) To allow for this type of effect all of the measured single-bead widths and dilutions were normalised to the average current, voltage and deposition rate readings for the corresponding multi-pass overlay. The normalised single-bead dilutions, D_n, were obtained by adapting the Bednarz-Deam model (see equation 2.2 – page 10), reported in Francis *et al.* (1998), and were given by:

$$\frac{D_n}{1-D_n} = \frac{\eta \frac{V_{ov} I_{ov}}{W_{ov}} \left(1 + \gamma V_{ov} I_{ov} S\right)}{\eta \frac{V_{sb} I_{sb}}{W_{sb}} \left(1 + \gamma V_{sb} I_{sb} S\right)} \times \frac{D_{sb}}{1-D_{sb}}$$

where the subscript *ov* denotes an average value of the parameter in the overlay and the subscript *sb* denotes an average value for the matching single-bead deposit. The normalised bead widths, w_n, were obtained using a similar procedure with equation 3.4:

$$w_n = \frac{\frac{C_1}{S} + C_2 V_{ov} I_{ov}}{\frac{C_1}{S} + C_2 V_{sb} I_{sb}} \times w_{sb}$$

A summary of the results is given in Table 6.3. Equation 6.13 (page 112) was used to predict the steady-state dilution. The steady-state penetration can be estimated if both the steady-state dilution and height are known. Penetration was used as the basis for all comparisons as it is the most sensitive indicator of the accuracy of a model.

Sample	Height, mm	Overlap	Inter-pass Temperature, (°C)	D_n	Predicted η (linear)	Penetration, mm	
						Predicted	Measured
A	2.0	0.48	Room	0.59	0.28	1.5	2.0
B	3.0	0.44	Room	0.48	0.21	1.5	1.5
C	4.3	0.50	Room	0.49	0.24	2.1	1.8
D	4.1	0.55	400	0.55	0.30	2.2	2.1
E	4.3	0.65	Room	0.49	0.32	1.4	0.9
F	4.3	0.69	400	0.59	0.40	1.9	1.3
G	5.2	0.62	Room	0.49	0.30	1.9	1.3
H	6.1	0.52	Room	0.45	0.24	2.4	1.7

Table 6.3: - A summary of results for the *k-η* model. The penetration refers to the average penetration of the overlay under steady-state conditions.

It is evident, from the results in Table 6.3, that a closer examination is required. The penetration is underestimated for the 2mm overlay and overestimated for overlays 5-6mm in height. The apparent dependence of average penetration on overlay height leads to the conclusion that the influence of overlay geometry may need investigation.

6.7 AN EMPIRICAL CORRECTION

A section through the 2mm high overlay sample was examined. One of the features of the penetration profile of a 2mm overlay can be seen in Figure 6.5. Eight beads were deposited in this overlay and the figure shows that there are also eight peaks in the penetration profile. It appears that as each subsequent bead is deposited a new peak in the penetration profile is created. For higher overlays this feature is often not present (see Figure 6.6). Thus, as a 2mm overlay is deposited, the melting front at the bottom of the weld pool must punch through the fusion line of the previous bead to create its own peak. Figure 6.7 illustrates how this punch-through effect results in more substrate being melted than equation 6.12 predicts and, therefore, how $\Box$ may be overestimated. The effect is pronounced when a thin overlay is deposited and the overlap is moderate to low. (It should be noted that low overlaps are generally required when depositing thin layers to ensure that the specified overlay height is not exceeded.)

For higher overlays the punch-through effect is generally not observed and in fact $\Box$ tends to be underestimated. In order to deposit a high overlay it is usually necessary to have a moderate-to-high overlap so that sufficient build-up of material is achieved. The combination of a high overlay and high bead overlap generally ensures that the current path between the tip of the electrode and the previous bead is somewhat shorter than the

path between the electrode and the substrate. Arc impingement and melting are thus biased toward the previous bead, causing η to assume a value that is higher than equation 6.12 predicts.

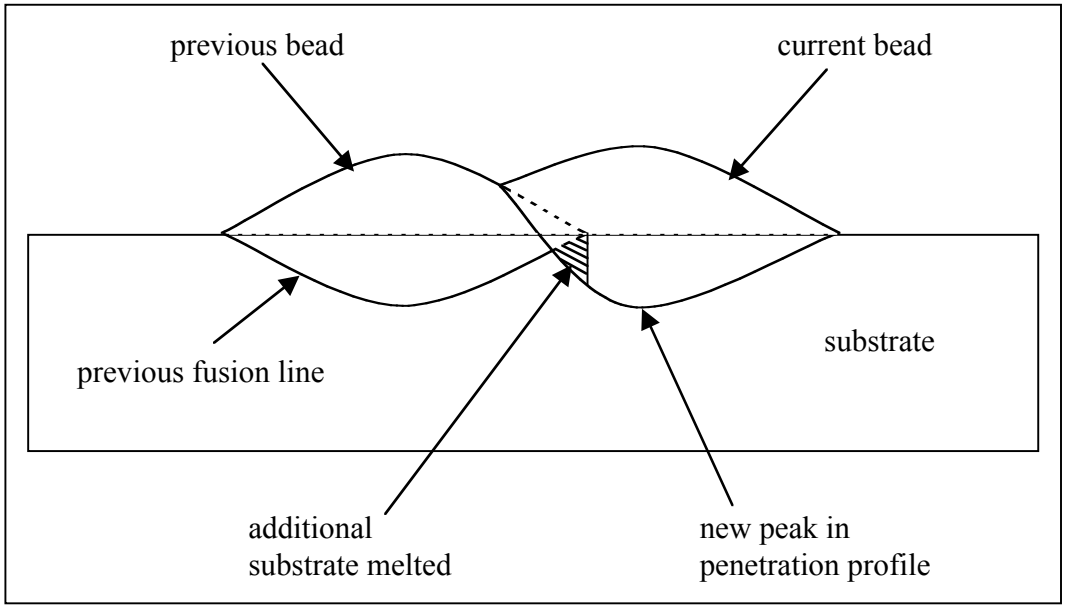

Figure 6.7: - Schematic representation of the punch-through effect in thin overlays. The fusion line of the current bead has "punched through" the fusion line of the previous bead to melt additional substrate material and create a new peak in the penetration profile. Deposition is proceeding from left to right.

Having identified how η may deviate from the values predicted by equation 6.12 it becomes possible to identify a suitable empirical correction. Equation 6.12 is a first order approximation; a straight line between two known end-points. Since the end-points are known to be correct, the correction must be such that it does not change the value of η at the end-points. The general form for such a correction is presented here:

$$\eta = \eta(1 - k) + a_1\eta(1 - \eta)(H_{ss} - a_2)(1 - k)$$

where H_{ss} is the steady-state overlay height in millimetres and a_1 and a_2 are fitted constants. The correction term is a quadratic function in Ω that maintains the end-point conditions. The (H_{ss} - a_2) component introduces a transition height (a_2) below which Ω is lower than the value predicted by equation 6.12 and above which it is higher. The least-squares best fit to the data in Table 6.3 is:

$$\Omega = \Omega(1 - k) + 0.254\Omega(1 - \Omega)(H_{ss} - 3.23)(1 - k) \quad \text{.....} \quad (6.15)$$

Thus the fitted transition height is 3.23mm. The experimental data are compared to the fitted results in Table 6.4. The fit for Ω is a least-squares best fit based on the error in steady-state penetration. It can be seen that there is a significant reduction in the discrepancies between the measured and predicted penetrations. The empirical correction reduces the inaccuracy that is seen at the extremes of the height range, and achieves an acceptable level of accuracy over the range of 2–6mm. Most single-layer overlays deposited in practice would fall in the range of 2–6mm.

It should be remembered that the analyses described in sections 6.2 to 6.5 were based on the assumption that Ω will have the same value for all beads in a multi-pass overlay. The height of a multi-pass overlay, however, changes from that of a single-bead deposit (*i.e.* the first bead) to the steady-state height. It would therefore appear that Ω will assume an initial value (corresponding to the second bead in the overlay) and then converge to a steady-state value as subsequent beads are deposited. Equation 6.15 is a least-squares best fit to the steady-state value of Ω and it is anticipated that, with the inclusion of the empirical correction, the *k*-Ω model will accurately predict the steady-state dilution for a

wide range of welding conditions. It is expected that the analyses described in earlier sections will serve as useful illustrations, and that the observed trends will still apply.

Sample	Height, (mm)	Overlap	Inter-pass Temperature, (^{o}C)	D_{sb}	δ (linear)	δ (fitted)	Penetration, mm	
							Predicted	Measured
A	2.0	0.48	Room	0.59	0.28	0.24	1.7	2.0
B	3.0	0.44	Room	0.48	0.21	0.21	1.6	1.5
C	4.3	0.50	Room	0.49	0.24	0.28	1.8	1.8
D	4.1	0.55	400	0.55	0.30	0.33	2.0	2.1
E	4.3	0.65	Room	0.49	0.32	0.35	1.2	0.9
F	4.3	0.69	400	0.59	0.40	0.44	1.5	1.3
G	5.2	0.62	Room	0.49	0.30	0.36	1.3	1.3
H	6.1	0.52	Room	0.45	0.24	0.32	1.5	1.7

Table 6.4: - Results from the *k*-δ model after an empirical correction was incorporated. The linear values of δ were obtained from equation 6.12 (page 111). The fitted values of δ were obtained from a least-squares best fit to equation 6.15.

6.8 REFINEMENT OF THE MODEL

In sections 6.2 to 6.6 the variables *k* and δ were assumed to remain constant, for a given set of welding conditions, from the first and second beads respectively until a steady-state condition was reached. In the previous section, however, it was suggested that δ could change as the overlay converges to the steady-state condition. In the transient region the composition of each successive bead will be different and so will be the thermal properties. Consequently *k* (which is dependent on thermal properties) may change too.

One parameter that is unlikely to vary significantly is the cross-sectional area of material deposited in each bead. In section 6.3 it was found that this parameter and the quantity of additional substrate melted per pass, under steady conditions, define the steady-state dilution. Thus, the k-α model revealed that analysing the beads in terms of their contributing area fractions was a valid approach, but also demonstrated that the choice of variables may not have been optimal. An analysis of multi-pass overlays is now presented in terms of the parameters that determine the steady-state dilution.

6.8.1 A New Variable, $\tilde{\alpha}$

Consider the case where a multi-pass overlay is being deposited. Each bead is deposited with identical welding parameters and a steady-state condition has been reached. With each pass a certain repeating cross-sectional area of substrate material is being melted. Let that repeating area be denoted by $A_{s(ov)}$ (see Figure 6.8). Consider also the deposition of a single bead with the same welding parameters. For the single bead a greater area of substrate, $A_{s(sb)}$, will be melted.

Let $\tilde{\alpha}$ be defined by the following relationship:

$$\tilde{\alpha} = \frac{A_{s(ov)}}{A_{s(sb)}} \quad \ldots\ldots \quad (6.16)$$

Thus $\tilde{\alpha}$ is the area of substrate melted per pass in an overlay under steady-state conditions, as a fraction of that melted in a matching single bead. This definition for $\tilde{\alpha}$ will be seen to be very useful.

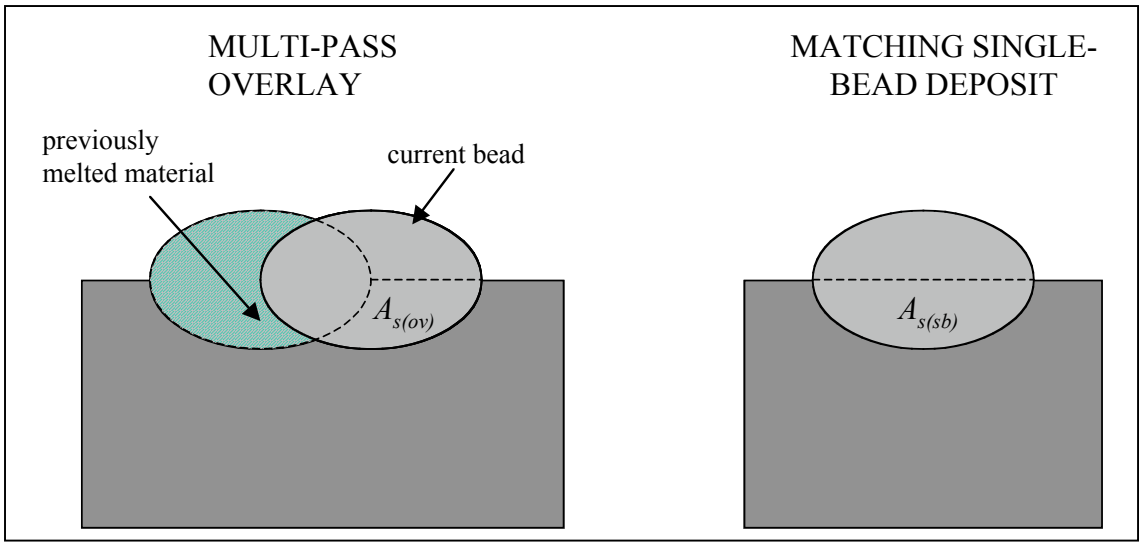

Figure 6.8: - A schematic representation of the repeating area of substrate, $A_{s(ov)}$, that is melted in each pass under steady-state conditions. $A_{s(sb)}$ represents the area of substrate that would be melted if a single bead were to be deposited under identical welding conditions.

6.8.2 Dilution of an Overlay

The cross-sectional area of material deposited in a single bead, A_d, is given by:

$$A_d = \frac{W}{\rho S} = A(1 - D_{sb}) \quad \ldots\ldots\ldots \quad (6.17)$$

where: W = deposition rate,

ρ = density of an all-weld-metal deposit,

S = travel speed,

A = cross-sectional area of the entire bead, and

D_{sb} = single-bead dilution $(0 < D_{sb} < 1)$

Rearranging gives the total cross-sectional area of the bead:

$$A = \frac{W}{\rho S} \frac{1}{(1 - D_{sb})}$$

For a single bead the area of melted substrate, $A_{s(sb)}$, is given by the product of the total bead area and the single-bead dilution:

$$A_{s(sb)} = \frac{W}{\Delta S}\frac{D_{sb}}{1-D_{sb}} \quad \cdots\cdots\cdots (6.18)$$

Now, using the definition for Δ an expression can be written for the repeating area of substrate melted, $A_{s(ov)}$, under steady-state conditions in a multi-pass overlay:

$$A_{s(ov)} = \frac{W}{\Delta S}\Delta\frac{D_{sb}}{1-D_{sb}}$$

This area is repeated every step-over, Δ, and dividing the repeating area by the step-over will give the average penetration of an overlay under steady-state conditions, P_{ss}:

$$P_{ss} = \left[\frac{W}{\Delta S\Delta}\right]\frac{D_{sb}}{1-D_{sb}} \quad \cdots\cdots\cdots (6.19)$$

If the term in brackets is compared with equation 5.5 it can be seen that this term is equivalent to the steady-state overlay height. Thus, equation 6.19 can be rewritten:

$$P_{ss} = H_{ss}\frac{D_{sb}}{1-D_{sb}} \quad \cdots\cdots\cdots (6.20)$$

Equation 6.20 can then be substituted into equation 5.1 (page 93), together with the steady-state overlay height, H_{ss}, to provide the steady-state dilution of an overlay, D_{ov}:

$$D_{ov} = \frac{\Delta D_{sb}}{\Delta D_{sb} + 1 - D_{sb}} \quad \ldots\ldots\ldots (6.21)$$

Unfortunately, γ is a complicated function of thermal properties, geometry and other parameters such as inter-pass temperature. The challenge in analysing single-layer multi-pass overlays is to identify a working approximation for the function for γ

The end-points for the function were considered. When the overlap is zero each weld pass will melt an amount of substrate that is equal to the amount melted in a single-bead deposit, *i.e.*:

$$\gamma(0) = 1$$

However, when the overlap is 100% one would not expect any new substrate material to be melted:

$$\gamma(1) = 0$$

Thus, a first-order approximation to the function for γ is:

$$\gamma = 1 - \omega$$

An empirical correction was incorporated in the same way as for γ. The general form chosen for the correction was:

$$\gamma = 1 - \omega - b_1 \omega(1 - \omega)(H_{ss} - b_2)$$

where H_{ss} is the steady-state overlay height in millimetres and b_1 and b_2 are fitted constant terms. The least-squares best fit to the results for the eight overlays described in Table 6.3 was:

$$\gamma = 1 - \omega - 0.254\omega(1 - \omega)(H_{ss} - 3.23) \quad \text{.....} \quad (6.22)$$

It can be seen that, with this form of expression for ϕ, the model is mathematically equivalent to the *k*-ϕ model. However, the overlay dilution is now stated in terms of a variable that has fundamental significance.

6.9 SUMMARY

A model has been developed for open-arc weld deposition of high-chromium white iron overlays. The model is based on the definition of two new variables, and the concept that a bead in a multi-pass overlay should be thought of in terms of its contributing fractions. The first variable is the area fraction of deposited material, *k*, and the second is the area fraction of overlap, ϕ.

In deriving the *k*-ϕ model is was assumed that:

- any differences between the thermal and physical properties of the overlay and base material could be ignored, and that
- *k* would remain unchanged from the first bead and ϕ would remain unchanged from the second bead until a steady-state condition was reached.

A corollary of the latter assumption is that *k* and ϕ are independent of the height of the overlay. (*k* and ϕ were assumed to remain constant despite the requirement that the overlay height change from that of a single-bead deposit to the steady-state overlay height.) Comparisons with experiments, however, revealed that ϕ does vary with the overlay height. An empirical correction was successful in allowing the model to predict the steady-state dilution of an overlay with reasonable accuracy. The model adequately describes the data for two different high-chromium, high-carbon welding consumables and it is anticipated that it will generally describe the data for similar consumables. The model may also be applicable to other alloy systems.

An algorithm for determining the steady-state overlay composition for a given set of welding parameters has been outlined. A spreadsheet for predicting overlay compositions is also described. The spreadsheet allows any combination of welding parameters to be compared and near-optimum conditions can now be readily identified. The spreadsheet has been developed and distributed to many interested parties in the Australian hardfacing industry. The current format of the spreadsheet and examples of the output it produces are included in Appendix 1.

The model suggests that, as the overlap increases, more beads need to be deposited before a steady-state condition is reached. It also reveals that the steady-state dilution is independent of the amount of the previous bead that is melted, and dependent only on the steady-state mixing ratio of material deposited to new substrate melted in each pass. Consequently, the model has been redefined in terms of a single new variable $\square$; a variable that has fundamental significance.